Optimization laser parameters to simulate solar cell degradation induced by space radiation

Sara AZIZ[1], Dalia EL-FIKY*,[1], Gad M. GAD[2], Ayman MAHROUS[3]

*Corresponding author
[1]NARSS – National Authority for Remote Sensing and Space Science,
23-josef-tito, new nozha, Cairo 11769, Egypt,
sara.ramadanaiz.93@gmail.com, daliaelfiky@gmail.com*
[2]Department of physics, HELWAN University,
Helwan, Cairo 11795, Egypt
[3]Space Environment group, Egypt japan university of science and technology,
Alexandria Governorate, Egypt

DOI: 10.13111/2066-8201.2021.13.2.18

Received: 15 January 2021/ Accepted: 11 May 2021/ Published: June 2021

Abstract: *Space radiation has a catastrophic impact on solar cells performance, appears as a degradation in their electrical and physical properties, this may cause a satellite failure; to overcome this issue, ground testing is required. In this paper, the pulsed laser was used as an alternative irradiation tool to induce degradation in solar cell performance in order to simulate the space radiation effect on solar cells. Firstly, the solar cells were irradiated with a wavelength of 532 nm at different locations, with the same power to optimize the most effective area to irradiation. Secondly, the solar cells were irradiated to the optimized location with different laser fluences; the results showed a degradation in electrical and physical performance. The amount of degradation is proportional to the laser fluence. Dark current voltage (DIV) curves have been measured before and after laser irradiation. Solar cell degradation rates have been calculated based on the Degradation coefficients (KL, RC) and electrical damage models.*

Key Words: *monocrystalline solar cell, space environment, Dark current, voltage (DIV) Curve, Pulsed laser*

1. INTRODUCTION

Highly energetic particles (protons, electrons, neutrons and heavy ions) can damage semiconductor materials by displacing atoms from their lattice [1]; for silicon, when the energetic particle collide with nuclei, Frenkel defects will be formed creating a vacancy (V) and an atom interstitial (I) making disorder in the lattice [2]. Those defects degrades the generation of the electron-hole pairs thus affecting on the recombination lifetime, and reduces the minority carrier lifetime[3], which in turn increase the series resistance and decreasing the shunt resistance of the Dark I-V Curve [4]. In this work the pulsed laser will be presented to simulate the same effect of energetic particles on solar cells.

The process of photon that induced degradation in a silicon cell was first reported by Staebler and Wronski in 1977 and is known as the Staebler-Wronski Effect (SWE). They reported a strong initial degradation of short circuit current. This is due to a reduced bulk

carrier lifetime increasing internal recombination [5]. It was later observed that the same process occurs to a limited extent in crystalline solar cells fabricated on Czochralski (CZ) wafers [6].

Two diode models were used to characterize the solar cell performance [7] shown in Fig. 1.

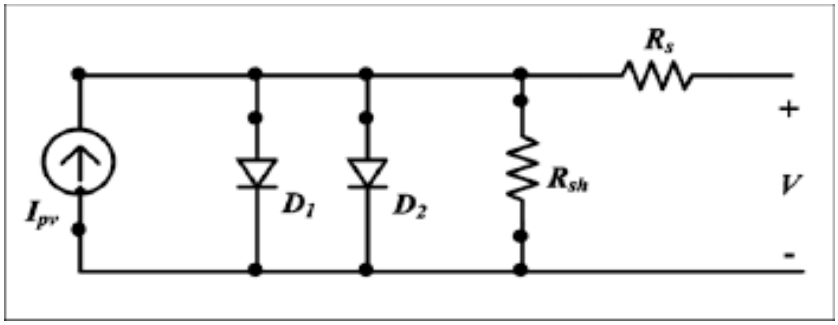

Fig. 1- Solar cell two diode model

Two-diode model is more accurate representation of solar cell behavior than the single-diode model [8]. The output parameters of the equivalent circuit for two models [9] are expressed by equations from (1-6).

$$Is = I(PV) - I(D1) - I(D2) - I(Rsh) \tag{1}$$

$$Is = I(PV) - I(\mathrm{D1})\left[\exp\left[\frac{q(V+IRs)}{KT} - 1\right]\right] - I(\mathrm{D2})\left[\exp\left[\frac{q(V+IRs)}{2KT} - 1\right]\right] - \frac{V+IRs}{Rsh} \tag{2}$$

$$ID1 = Io(\exp\frac{qv}{kt} - 1) \tag{3}$$

$$ID2 = Io(\exp\frac{qv}{2kt} - 1) \tag{4}$$

$$Rs = \frac{v}{Id1} \tag{5}$$

$$Is = I(PV) - I(D1) - I(D2) - I(Rsh) \tag{6}$$

where: *Is*: - the terminal current, *I*(*PV*): - the cell generated photocurrent, *I*(*D*1) & (*D*2): - First and second diode currents, *I*(*Rsh*): -shunt *Rs*: Series Resistance, *Rsh*: Shunt resistance: Boltzmann constant *T*: -Absolute Temperature.

The basic equations of the solar cell can be used to describe the changes which occur during irradiation, the required data refer to the series resistance, shunt resistance, and the basic diode parameters of saturation current and diode quality factor defined as (*Rs*, *Rsh*, *Id*1, *Id*2, n1 and n2, respectively).

Analyzing the changes of the DIV parameters before and after irradiations helps in identifying the defects in the monocrystalline solar cell [10].

As shown in fig 2, the electrical performance of the solar cell could be defined according to degradation modes of the DIV curve; based on DIV curve measurements before and after pulsed irradiation, the reason of degradation will be illustrated. An increase in the series resistance and a decrease in the shunt resistance indicate a degradation in the solar cell electrical performance.

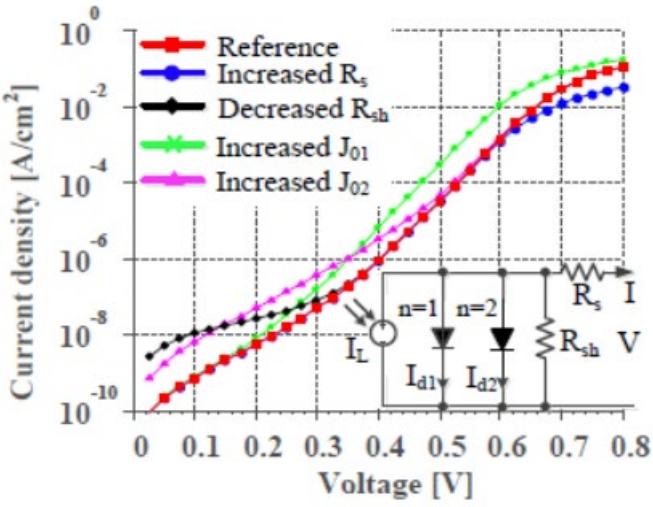

Fig. 2 - Dark-Current voltage (DIV)curve of the solar cell with different degradation mode

It will be possible to identify why a device is underperforming by indicating External Quantum efficiency (EQE) [11] that defines the state of the solar cell. Studying the physical parameters as diffusion length, carrier concentration and recombination we are able also to know the functionality of the semiconductor devices. The value of minority carrier's life time is used to estimate the solar cell performance; it could be measured with the formula in equation (7) [12].

$$\tau = \frac{\Delta n}{R} \tag{7}$$

where: - τ is the minority carrier lifetime, Δn is the excess minority carrier's concentration and R is the recombination rate.

It is important to characterize the solar cell damage in the term of change in diffusion length since the diffusion length can measure the amount of degradation in the base layer, which caused by the laser fluence, i.e the fluence as a function of the damage coefficient must be determined. The output parameters of the solar cell as a function of the fluence could be described statically as the change in the minority carrier diffusion length, L, as a function of fluence (Ø) [13]. In accordance with equation (8).

$$\Delta\frac{1}{L^2} = \frac{1}{L^2(\emptyset)} - \frac{1}{(L^2)\Theta} = \Sigma\frac{ln\sigma i\, \upsilon\emptyset}{D} = K(L)\,\emptyset \tag{8}$$

where $L^2(\emptyset)$ is the diffusion length after Irradiation, $(L2)$ Ø is the diffusion length before Irradiation, ln represents the introduction rate of recombination centers by radiation, σi is the capture cross section of minority carrier by recombination center, υ is the thermal velocity of the minority carrier, D represents the Minority carrier diffusion coefficient, $K(L)$ is the Damage coefficient for the minority carrier diffusion length and Ø represents the fluence of the radiation. The change of the carrier concentration base as a function of fluence[14] can be expressed by using equation (9), where $P\Theta$ is the carrier concentration before irradiation, $P(\emptyset)$ is the carrier concentration after irradiation and Rc, is the carrier removal rate [14].

$$\Delta P\emptyset = P\Theta\, e^{\frac{-Rc\emptyset}{P\Theta.}} \tag{9}$$

It is possible to evaluate the solar cell radiation effects in terms of common engineering output parameters. The variation of common solar cell output parameters during irradiation can be described in terms of *Isc*, Vop, Pmax with the fluences according to equations from (10 - 12).

$$Isc = Isc0 - C\log(1 + \emptyset) \quad (10)$$

$$Voc = Voc0 - C' \log(1 + \emptyset) \quad (11)$$

$$Pmax = Pmax0 - C'' \log(1 + \emptyset) \quad (12)$$

where C constant represents the decrease in Isc per decade in radiation fluence' constant represents the increase in Voc per decade in radiation fluence, C'' constant represents the decrease in the output power per decade in radiation fluence (Isc, Vop and Pmax) respectively, $\emptyset$ represents the radiation fluence at which the electrical parameter start to degrade.

The fitting parameters as a function of displacement damage dose is given in the Solar Cell Radiation Handbook[15].

Upon a numerical data fit, the following values for the constants were determined: A=4.76 (%), C= 1.353 (%I, and D,= 1 .433(MeV/g).within const in ranges. Physical characterization of irradiated solar cell and the electric degradation performance after pulsed laser irradiation are investigated by using PC1D software.

The PC1D computer program [16] which solves the fully coupled nonlinear equations for quasi one-dimensional transport of electrons and holes in crystalline Si device, was applied to calculate the physical characteristics based on simulation of the solar cell structures and measured Dark I-V of solar cell.

2. EXPRIMENTAL WORK

Pulsed Laser System (PLS) Facility, is located at the National Authority for Remote Sensing and Space Science (NARSS) Cairo, Egypt, the system shown in Fig. 3. The pulsed laser system has been supplied with Nd-YAG Solid State Laser Crystal that work as amplifier of the laser. The full system is automated to scan the laser spot over a predefined region by the lab-VIEW software. Also, the pulsed laser beam diameter is focused to get the same effect of energetic particle by using a microscope and a CCD camera. The beam before microscope was 3 mm and after microscope become 1 μm and that is very useful for increase the laser beam damage effect on the solar cell. In this system, There are two wavelengths 1064 nm and 532nm. In this research PLS initializes the same effect induced by energetic particles on the solar cells; Solar cell irradiated with laser beam parameters are (532 nm,1000 Hz, 1μm) for (Wavelength, repetition rate, beam diameter), respectively.

The second harmonic generation (532 nm) is a shorter wave length than the infra-red (1064)nm. Based on that ,the second harmonic generation has been chosen because short wave length is able to penetrate the silicon material of the solar cell and cause bulk defects in the solar cell [16].

The required energy to displace one atom from the silicon material is at least 21 eV energy; this effect is called Primarily knock on atom (PKA) [18] and the required energy for the solar cell irradiation must be greater than the band gab energy of the silicon. Based on that, the first energy level of the pulsed laser is approximately 9 Mev; this energy is determined by considering the laser pulse as a group of photons per sec [19] [20]; to transfer the incident radiation energy to the lattice the laser pulse must be greater than 10 picosecond [21], the time duration of the laser is (12 Ps).

Fig. 3 - Picosecond pulsed laser system (PPLS).

The experimental work was performed with a commercial Mono-crystalline solar cell; its efficiency ranges between 21% -25%. The Area is 32 cm^2, the electrical parameters of the mono-crystalline solar cell as shown in its Data sheet is presented in Table 1.

Table 1 - solar cell electrical parameters

Parameter	V_{oc}	I_{sc}	I_{MP}	V_{MP}	P_{max}
Value	0.618	1.127 A	0.9763	0.4525 V	0.4313W

Mono-Crystalline solar cells samples used in the current study have the same electrical and physical parameters. Firstly, the solar cells Exposure to different locations (Rear side to Edge parts), (Front Side to Edge parts), (Front side to centre parts) and (Rear side to centre parts). All solar cells will be exposed with the same laser parameters (532 nm ,1.378 mw) for (Wavelength, power). The cell area is divided into six rectangles as shown in Fig. 4 where Edge position means pulsed laser beam scans rectangles (1, 2, 3, 6) with yellow colour in Fig. 4 with an area of 22 cm^2 and Centre position means the pulsed laser beam scans rectangles (4,5) with an area of 10 cm^2. Secondly, solar cells were irradiated at room temperature with four different laser fluences (2.1×10^{19}), (2.29×10^{19}), (2.6×10^{19}) and (3×10^{19}), photons/ cm^2. Laser fluence is defined as the number of photons per irritated area which corresponds to the effective focal length.

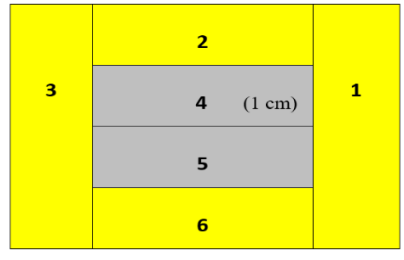

Fig. 4 - Solar cell area divided to 6 rectangles

For the DIV measurement, the Electronic Circuit had been designed at space environment lab. The circuit diagram is shown in Fig. 5 and the circuit design is shown in Fig. 6; output data of current and voltage are saved on the Computer for plotting DIV. The electrical properties of solar cells are observed with the Dark I-V, Illumination I-V and quantum efficiency (QE). The solar cell structure was simulated with PC1D5 software. The theoretical

device was defined matching the experimental electrical parameters.PC1D was previously used to investigate the effect of the radiation damage on silicon solar cells [22], [23].

The Dark I-V parameters were calculated and then used as input in the one-dimensional simulator (PC1D).

The outputs of the PC1D software are Quantum Efficiency (QE), surface recombination, the P-type and N-type doping concentration and diffusion length. Theses parameters are used to show the changes that happened in the physical characterization of the solar cell after the laser irradiation process.

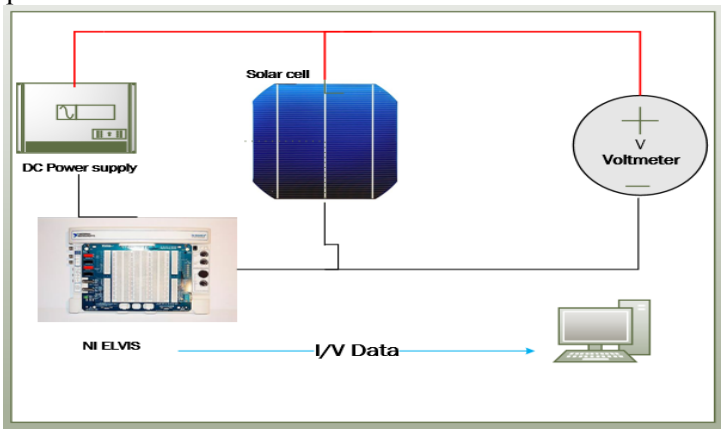

Fig. 5 - Electronic circuit for measure DIV curve

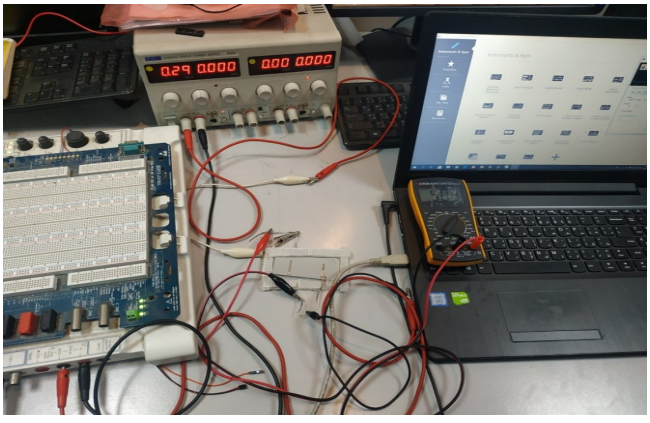

Fig. 6 - Circuit design at space Environment lab for DIV measurements

3. RESULT AND DISCUSSION

Exposure to Rear side Edge parts

Fig. 7 shows no change in the solar cell electrical performance after the exposure to the Rear side Edges parts with the second harmonic wave length (532 nm).

This due to there is a very low current at edges of solar cell, because of solar cell edge recombination [24].

Additionally, the rear side of solar cell hasn't any grid contact so the ultrashort pulsed laser beam has no significant effect on the performance of the solar cell within to exposure to edge parts rear side.

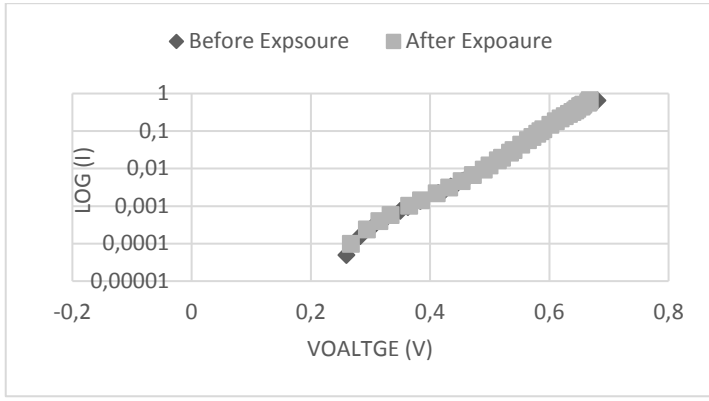

Fig. 7 - DIV before and after irradiation to Rear side Edge parts with wave length (532) nm and power 1.378 mW

Exposure to Front side edge parts

Fig. 8 and Table 2 show the degradation performance of the dark I-V curve after the irradiation to Front side Edges area. That can be illustrated by the decreasing in shunt resistance, increasing in series resistance and increasing in leakage current value. Those effects are annihilated after several hours.

This temporary degradation can be attributed to the heat effect of pulsed laser beam, as the saturation current density is function of solar cell temperature [25].

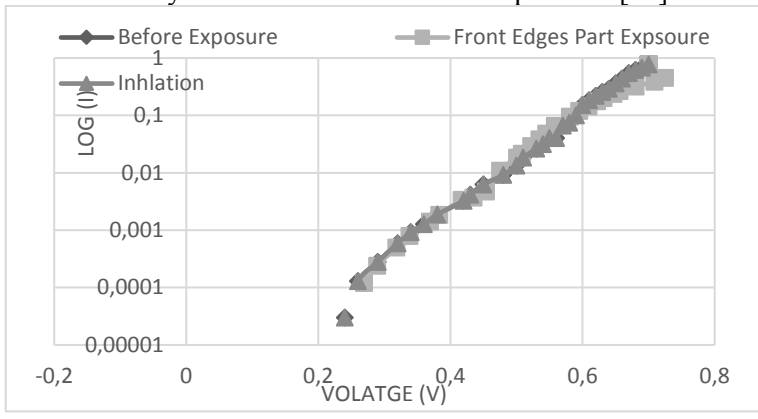

Fig. 8 - DIV before and after irradiation to front side edge parts with 532 nm and 1.378 mw

Table 2 - DIV parameters before and after irradiation to front side with 1.378 mW power

Parameter	Before Exposure	After exposure
(R_{sh}) Ω	256.4	285.7
(R_{s}) Ω	0.1233	0.39
(I_{s1}) A	2.00E-06	0.00001
(I_{s2}) A	1.00E-07	3E-07
n_1	1.6	1.6
n_2	2.177	2.1536
I_{Sc} (A)	1.127 A	1.088
V_{oc}(V)	0.6180	0.6101
P_{max}(W)	0.4313 W	0.3048

Physical parameters for exposure to front side edge parts are shown in Table 3; the data showed an increase in the speed of the electron-hole pairs in front surface recombination from

30000 to 54000 cm/s and a reduction in the recombination life time from 30 to 20 us. The front side of the solar cell absorbed the short wave length, and the laser beam increases the generation of electron-hole pairs and increased the surface speed recombination. After several hours the solar cell parameters returned back to its original values. Within the exposure to Front Side Edge Parts, the effect pf the pulsed laser was thermal effect not bulk damage.

Table 3 - Physical parameters output of the solar cell before and after exposure to front side edges parts by PC1d software

Physical Parameters	Before Exposure	After Exposure
Base Contact	0.15 Ω	0.25
Internal Conductor	1×10^{-3}	8×10^{-3}
P-Type Doping (cm^{-3})	1×10^{16}	$1x10^{16}$
N-Type Doping (cm^{-3})	1×10^{19}	1×10^{19}
Bulk Recombination	30 us	20 us
Front Surface Recombination (cm/s)	Sn=Sp=30000	Sn=Sp=45000
Rear Surface Recombination (cm/s)	Sn=Sp=100	Sn=Sp=100

Exposure front side center parts

In case of exposure the solar cell to front side to center parts, DIV before and after exposure is shown in Fig. 9. An obvious decrease in the shunt resistance without annihilation. Table 4 showed a low decrease in shunt resistance, without change in series resistance and no increase in saturations current.

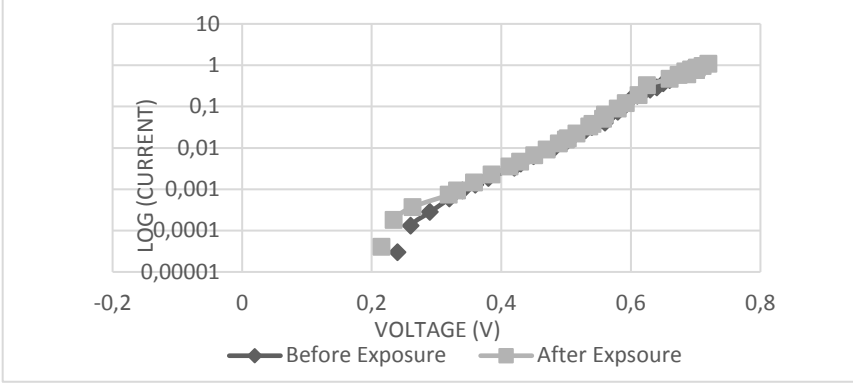

Fig. 9 -DIV before and after irradiation to front side center parts with 532 nm and 1.378 m

Table 4 - DIV parameters before and after irradiation to front side with 532 nm wave length and 1.378 mW power

Parameter	Before Exposure	After Exposure
(R_{sh}) Ω	322.58	303.03
(R_s) Ω	0.125	0.125
(I_{s1}) A	2.00E-06	2.00E-06
(I_{s2}) A	3.00E-07	5.00E-08
n_1	1.7	1.668
n_2	2.0	2.2
I_{Sc} (A)	1.127 A	0.946

V_{oc}(V)	0.6180	0.6184
P_{max}(W)	0.4313 W	0.3650

Table 5 shows the change in physical parameters after pulsed laser irradiation for front center parts. As the second harmonic, the data show a change in the P-doping concentration from 1×10^{16} to 2.8×10^{16} that shows the laser beam change in the material itself and that change was not temporary.

Table 5 - physical parameters output of the solar cell before and after exposure to front side center parts by PC1d software

Physical Parameter	Before Exposure	After Exposure
Base Contact	0.13 Ω	0.15
Internal Conductor	1×10^{-3}	0.02
P-Type Doping (cm^{-3})	1×10^{16}	2.8×10^{16}
N-Type Doping (cm^{-3})	1×10^{19}	1×10^{19}
Bulk Recombination	30 us	10 us
Front Surface Recombination (cm/s)	Sn=Sp=30000	Sn=Sp=40000
Rear Surface Recombination (cm/s)	Sn=Sp=100	Sn=Sp=100

Exposure to Rear side to center parts

Fig. 10 and Table 6 show the degradation in the electrical parameters after irradiation to the Rear side Center parts where the shunt resistance decreased and the series resistance increased without annihilation.

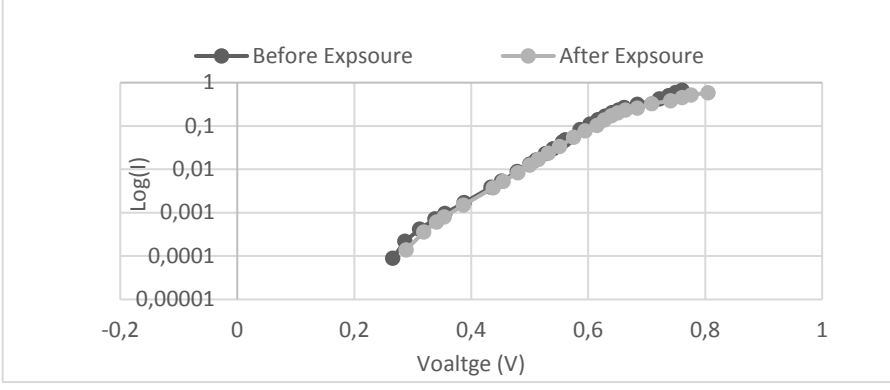

Fig. 10 - DIV before and after laser irradiation to rear side center parts with 1.378 mW

Table 6 - DIV parameters before and after irradiation to rear side center parts with 1.378 mW

Parameter	**BEFRE EXPOSURE**	**AFTER EXPSOURE**
(R_{sh}) Ω	434.7	384.615
(R_{s}) Ω	0.227	0.3519
(I_{s1}) A	5E7	8E7
(I_{s2}) A	1.00E5	1.00E5
n1	2.00	2.1
n2	2.5	2.56
I_{Sc} (A)	1.127 A	1.040
V_{oc}(V)	0.6180	0.5845
P_{max}(W)	0.4313 W	0.3158

The physical parameters in Table 7 shows a high decrease in the recombination life time with an observed change in P-type doping concentration.

Table 7 - Physical parameters before and after irradiation to rear side center parts with 532 NM wave length and 1.378 mW power

Physical Parameter	Before Exposure	After Exposure
Base Contact	0.15	0.2
Internal Conductor	0.001	0.01
P-Type Doping	1*E16	8×10^{15}
Bulk Recombination	30 µs	4.5 µs
Rear Surface Recombination	Sn=Sp=30000	Sn=Sp=45000

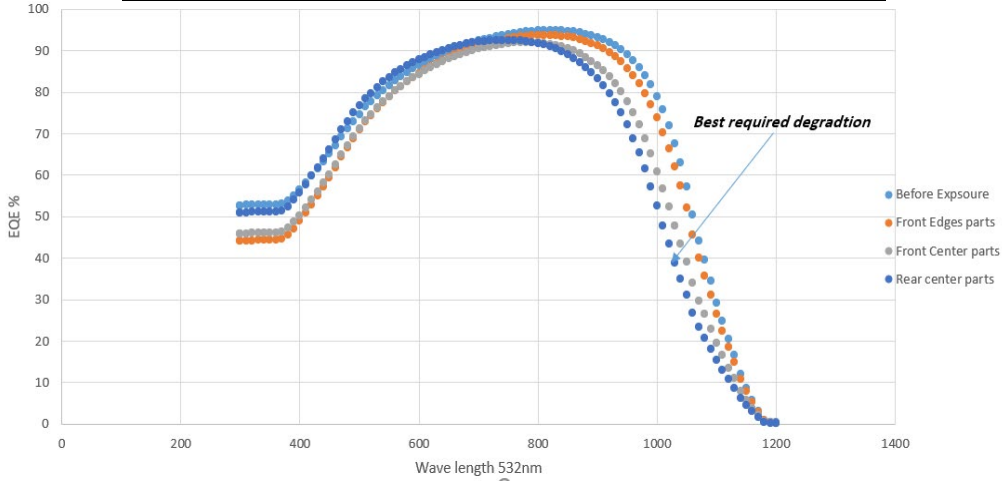

Fig. 11 - EQE for different exposure locations

Fig. 11 show the change of EQE of Si solar cell with expose to different locations (front edge parts-front center parts and rear center parts). In case front side edge parts, the effect of pulsed laser was temporary (Thermal damage). There was a magnificent decrease in the EQE and after several hours the curve inhaled to its original. For the exposure to center parts in the rear and front side, the degradation was due to change in the carrier concentration and recombination life time. Then the effect of pulsed laser was permanent (Bulk damage). The degradation level in the EQE of the rear side center parts was greater than the front side center parts. Based on that, the optimum location for laser beam exposure with lowest is "Rear Side Center Parts" of solar cell with area 10 cm^2.This location absorbs the wave length (532)nm (short wave length) , and this wave length penetrate the solar cell structure making defects in the solar cell structure with lowest power. From all previous presented results, the optimum conditions and parameters to induce degradation in solar cell using pulsed laser beam, exposure the solar cell from rear side center parts, at 532nm wavelength with threshold power (1.378mW), Beam diameter(1µm), reptation rate (1000 Hz) and duration (25 pico-second). Secondly, solar cell irradiated to the optimum location with different fluence of pulsed laser.

Current–voltage (I–V) and spectral response measurements were taken for each cell and fluence. The QE and remaining factor for Isc, Voc, and Pmax were obtained experimentally as functions of laser fluence. Figure (10) shows the effect of pulsed laser fluence on the I-V curve of the solar cell, with powers (1.29, 1.378, 1.5239, 1.6923) mW the different fluences are different laser fluences (2.1×10^{19}), (2.29×10^{19}), (2.6×10^{19}) and (3×10^{19}), the first power was lower than the previous study, this power increased the solar cell power from its initial

value, the power was able to ionize the semiconductor material forming electron hole-pairs and increased the efficiency and as laser fluence increase the power of the solar cell decreased as shown in Table 8.

Table 8 - Electrical characterization of monocrystalline solar cell with change of pulsed fluence

Parameter	**V_{oc} (v)**	**I_{sc}(A)**	**P_{max}(W)**
Before Exposure	0.6180	1.127	0.4313
Fluence (2.1×10^{19})	0.6312	1.0086	0.4084
Fluence (2.92×10^{19})	0.5845	1.040	0.3158
Fluence (2.6×10^{19})	0.5695	1..010	0.2943
Fluence (3×10^{19})	0.2197	0.973	0.2197

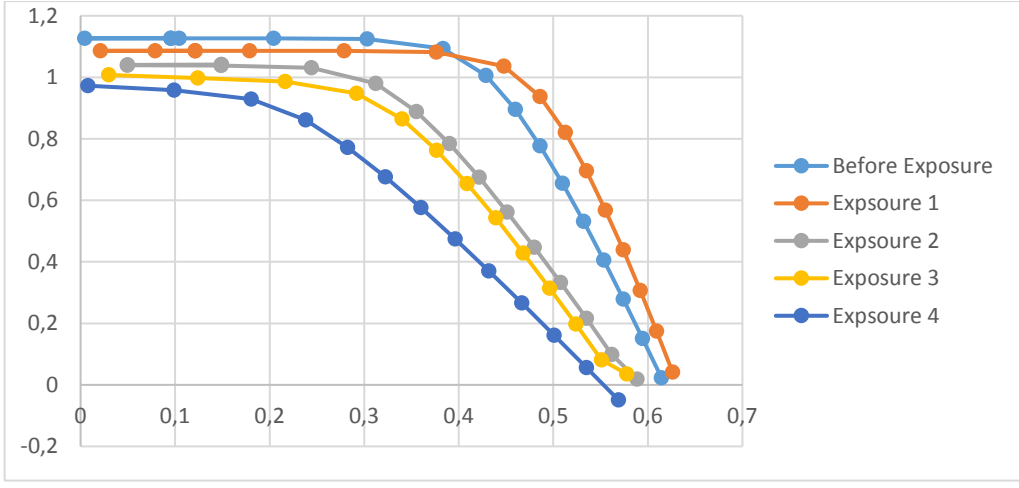

Fig. 12 - I - V curve variation of the solar cell with change of the laser fluence (2.1×10^{19}), (2.29×10^{19}), (2.6×10^{19}) and (3×10^{9})

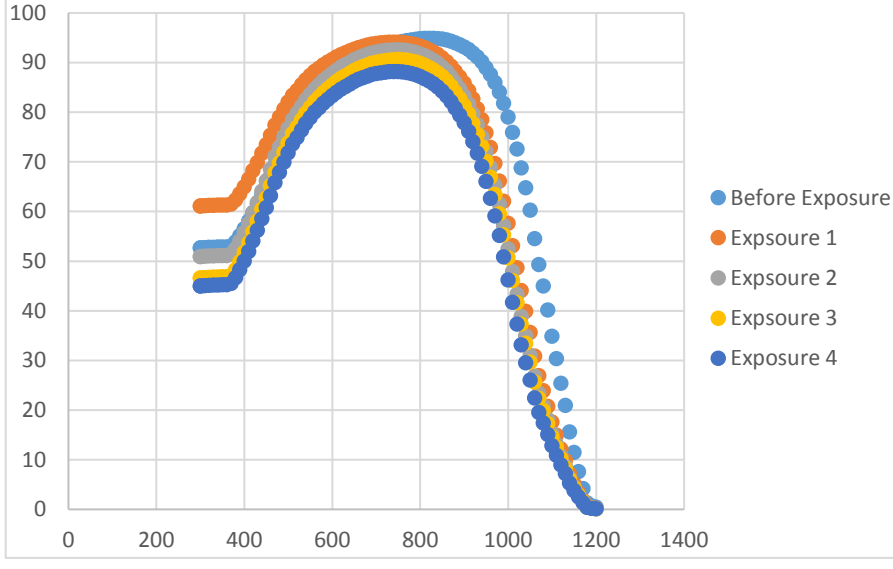

Fig. 13 -EQE of monocrystalline solar cell with respect to different laser fluences (2.1×10^{19}), (2.29×10^{19}), (2.6×10^{19}) and (3×10^{19}), (photons/cm^2)

In order to calculate the damage parameters of the effect of the laser on the solar cell, carrier remover rate (Rc) and the Damage coefficient for the minority carrier diffusion length (Kl), we will use equations (8,10).in fitting graph Fig. 14 and Fig. 15. The effect of irradiation upon the carrier concentration is clearly illustrated in Fig. 14. As laser fluence increases, the carrier concentration decreases; the carrier concentration damage coefficient (Rc) was determined using eq. 9. The career concentration remover rate was 0.005cm^{-1}.

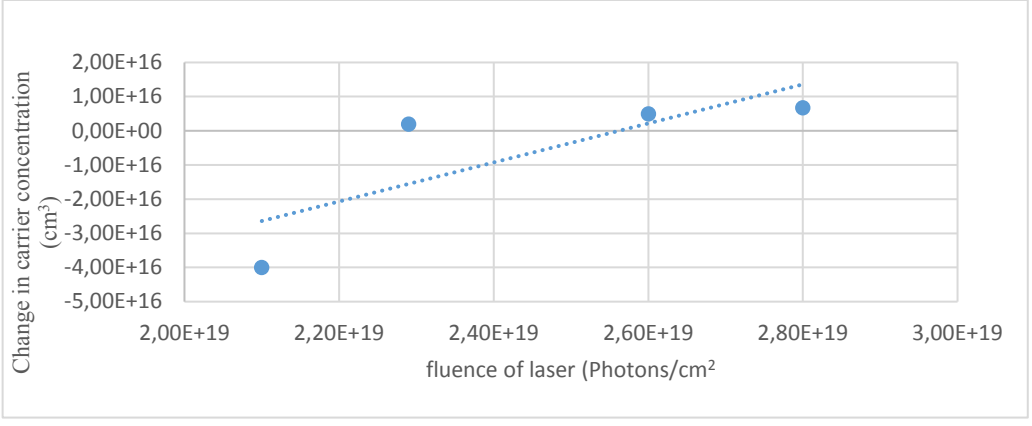

Fig. 14 - Variation of the base carrier concentration of the base carrier as a function laser fluence (2.1×10^{19}), (2.29×10^{19}), (2.6×10^{19}) and (3×10^{19}) (photons/cm^2)

In Fig. 15 As laser fluence increase the minority carrier diffusion length increase, which implies the degradation increased with increasing the fluence. Minority carrier damage coefficient (KL) was determined using eq. 8 to be 6E-24 cm^{-3}. Damage constants Kl for 1 MeV electron irradiated silicon solar cell is determined to be used in the prediction of the solar cell performance [26].

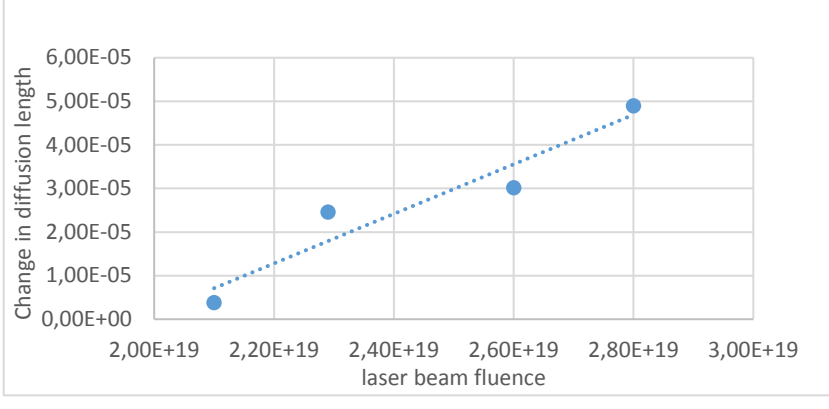

Fig. 15 - Changes in the inverse square of diffusion length as a function with laser fluence fluence (2.1×10^{19}), (2.29×10^{19}), (2.6×10^{19}) and (3×10^{19}) photons/cm^2)

Fig (16) shows the degradation curves of remaining factors to Isc, Pmax, and Voc as a function of laser fluence. The remaining factor of the vertical axis is defined as the ratio of the value After laser irradiation. Isc decreased with the fluence, and increased in the Voc which in turn showed a sharp degradation in Pmax. To describe this radiation damage quantitatively, the fitting parameters were measured with respect to equation from (10-12) as given in the Solar Cell Radiation Handbook. (C, C' and C)"'approaches to (1.2388, 1.3453 and 3.0897) mA/cm^2 respectively.

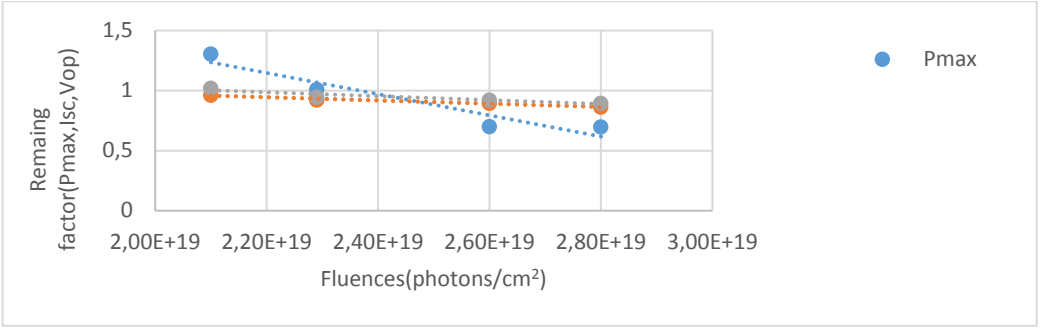

Fig. 16 - Variation of Remaining fraction of output parameters (Isc, Vop, Pmax) with the laser fluence

4. CONCLUSIONS

In order to simulate the effect of the space radiation on the solar cells, Picosecond Pulsed laser was used to induce permeant damage in the solar cell structure; to achieve that, firstly, the optimization of the laser exposure conditions is determined; the results of DIV parameters and PC1d software showed the optimum location of the exposure that induce a stable degradation is the rear side to center parts of the solar cell. The laser parameters of the exposure are defined as wavelength, beam diameter, threshold power, reputation Rate and pulsed duration (532 nm), (1μm), (1.327mW), (1000Hz) and (25Ps), respectively. Secondly, the solar cells irradiated with the pulsed laser in the optimum location with different laser fluences (2.1×10^{19}), (2.29×10^{19}), (2.6×10^{19}) and (3×10^{19}) (photons /cm^2). The experimental results of the electrical parameters before and after the laser irradiation are presented. An analytical model for radiation damage by pulsed laser to solar cells based on the damage constant for lifetime and carrier removal rate of solar cell materials has been proposed. The results showed a correlation with the previous studies of the effect of the energetic particles on the solar cells, with this analytical result and its validations with predication models under the effect of electrons and protons fluences; then we were able to simulate the space radiation induced damage in solar cell by the picosecond pulsed laser. This paper provides an understanding and estimating the effects of pulsed laser on the solar cell, obtaining optimal procedure of irradiation and determination of degradation coefficients of laser irradiation. And that are beneficial and the most practical way to present the pulsed laser system (PLS) as alternative tool for testing the space solar cells before lunching.

REFERENCES

[1] J. R. Srour, C. J. Marshall, and P. W. Marshall, Review of displacement damage effects in silicon devices, *IEEE Transactions on Nuclear Science*, vol. **50**, no. 3, pp. 653–670, Jun. 2003, doi: 10.1109/TNS.2003.813197.

[2] P. V. Dressendorfer, *Basic mechanisms for the new millennium*, Sandia National Labs., Albuquerque, NM (United States), SAND-98-1388C; CONF-980705-, Sep. 1998. Accessed: Dec. 26, 2020. [Online]. Available: https://www.osti.gov/biblio/658465-basic-mechanisms-new-millennium

[3] S. Duzellier, Radiation effects on electronic devices in space, *Aerospace Science and Technology*, vol. **9**, no. 1, pp. 93–99, Jan. 2005, doi: 10.1016/j.ast.2004.08.006.

[4] K. Bouzidi, M. Chegaar, and M. Aillerie, Solar Cells Parameters Evaluation from Dark I-V Characteristics, *Energy Procedia*, vol. **18**, pp. 1601–1610, 2012, doi: 10.1016/j.egypro.2012.06.001.

[5] * * * Staebler-Wronski Effect - an overview | ScienceDirect Topics. https://www.sciencedirect.com/topics/chemistry/staebler-wronski-effect (accessed Jan. 13, 2021).

[6] B. Sopori, T. Tan, and P. Rupnowski, Photovoltaic Materials and Devices, *International Journal of Photoenergy*, May 30, 2012, https://www.hindawi.com/journals/ijp/2012/673975/ (accessed Dec. 27, 2020).

[7] T. Nguyen-Duc, H. Nguyen-Duc, T. Le-Viet, and H. Takano, Single-Diode Models of PV Modules: A Comparison of Conventional Approaches and Proposal of a Novel Model, *Energies*, vol. **13**, no. 6, Art. no. 6, Jan. 2020, doi: 10.3390/en13061296.

[8] N. Mohamed, N. Z. Yahaya, and B. Singh, *Single-diode model and two-diode model of PV modules: A comparison*, 2013, p. 214. doi: 10.1109/ICCSCE.2013.6719960.

[9] H. Abunahla and S. Mahmoud, Modeling and Simulation of Photovoltaic Modules, 2013.

[10] S. V. Spataru, D. Sera, P. Hacke, T. Kerekes, and R. Teodorescu, Fault identification in crystalline silicon PV modules by complementary analysis of the light and dark current–voltage characteristics, *Progress in Photovoltaics: Research and Applications*, vol. **24**, no. 4, pp. 517–532, 2016, doi: https://doi.org/10.1002/pip.2571.

[11] W. Ananda, *External quantum efficiency measurement of solar cell*, 2017, p. 456. doi: 10.1109/QIR.2017.8168528.

[12] Sinton and R. M. Swanson, Recombination in highly injected silicon, *Electron Devices, IEEE Transactions on*, vol. **34**, pp. 1380–1389, 1987.

[13] M. Yamaguchi, S. J. Taylor, S. Matsuda, O. Kawasaki, and K. Ando, Analysis of damage to silicon solar cells by high fluence electron irradiation, in *Conference Record of the Twenty Fifth IEEE Photovoltaic Specialists Conference - 1996*, Washington, DC, USA, 1996, pp. 167–170. doi: 10.1109/PVSC.1996.563973.

[14] S. Messenger, E. Jackson, E. Burke, M. Xapsos, and G. Summers, Structural changes in InP/Si solar cells following irradiation with protons to very high fluences, *Journal of Applied Physics - J APPL PHYS*, vol. **86**, pp. 1230–1235, Aug. 1999, doi: 10.1063/1.370876.

[15] T. Markvart, Radiation damage in solar cells, *J Mater Sci: Mater Electron*, vol. **1**, no. 1, pp. 1–12, May 1990, doi: 10.1007/BF00716008.

[16] M. Belarbi, A. Benyoucef, and B. Benyoucef, Simulation of the solar cells with PC1D, application to cells based on silicon, *Advanced Energy: an International Journal*, vol. **1**, pp. 1–10, Jul. 2014, doi: 10.5121/aeij.2014.1301.

[17] S. Buchner, D. McMorrow, J. Melinger, and A. B. Camdbell, Laboratory tests for single-event effects, *IEEE Transactions on Nuclear Science*, vol. **43**, no. 2, pp. 678–686, Apr. 1996, doi: 10.1109/23.490911.

[18] B. J. Cowen and M. S. El-Genk, Point defects production and energy thresholds for displacements in crystalline and amorphous SiC, *Computational Materials Science*, vol. **151**, pp. 73–83, Aug. 2018, doi: 10.1016/j.commatsci.2018.04.063.

[19] * * * T*ech note for pulsed beam characterization.pdf*, Accessed: Dec. 26, 2020. [Online]. Available: http://www.sal.wisc.edu/PFIS/docs/rss-vis/archive/protected/pfis/3150/laser%20cutter/Tech%20note%20for%20pulsed%20beam%20characterization.pdf

[20] M. Young and R. A. Lawton, *Measurement of pulsed-laser power*, National Bureau of Standards Technical Note 1010, Nat. Bur. Stand. (U.S.), Tech. Note 1010,40 pages (Feb.1979), p. 42.

[21] B. C. Stuart, M. D. Feit, A. M. Rubenchik, B. W. Shore, and M. D. Perry, Laser-induced damage in dielectrics with nanosecond-to-subpicosecond pulses, in *Conference on Lasers and Electro-Optics (1995), paper CFD2*, May 1995, p. CFD2. Accessed: Jan. 13, 2021. [Online]. Available: https://www.osapublishing.org/abstract.cfm?uri=CLEO-1995-CFD2

[22] A. Ouedraogo, L. Mogmenga, N. Bado, T. S. M. Ky, and D. J. Bathiebo, Analysis of the Single-Crystalline Silicon Photovoltaic (PV) Module Performances Under Low γ - Radiation from Radioactive Source, *Silicon*, vol. **12**, no. 8, pp. 1831–1837, Aug. 2020, doi: 10.1007/s12633-019-00282-7.

[23] M. Imaizumi, M. Yamaguchi, S. J. Taylor, S. Matsuda, O. Kawasaki, and T. Hisamatsu, Mechanism for the anomalous degradation of Si solar cells induced by high-energy proton irradiation*Solar Energy Materials and Solar Cells*, vol. 50, no. 1, pp. 339–344, Jan. 1998, doi: 10.1016/S0927-0248(97)00164-5.

[24] A. Fell, J. Schön, M. Müller, N. Wohrle, M. Schubert, and S. Glunz, Modeling Edge Recombination in Silicon Solar Cells, *IEEE Journal of Photovoltaics*, vol. PP, pp. 1–7, Jan. 2018, doi: 10.1109/JPHOTOV.2017.2787020.

[25] P. Singh and N. M. Ravindra, Temperature dependence of solar cell performance—an analysis, *Solar Energy Materials and Solar Cells*, vol. **101**, pp. 36–45, Jun. 2012, doi: 10.1016/j.solmat.2012.02.019.

[26] M. Yamaguchi, A. Khan, S. J. Taylor, M. Imaizumi, T. Hisamatsu, and S. Matsuda, A detailed model to improve the radiation-resistance of Si space solar cells, *IEEE Transactions on Electron Devices*, vol. **46**, no. 10, pp. 2133–2138, Oct. 1999, doi: 10.1109/16.792008.